Journal of Environmental Health Science and Engineering (2020) 18:35–50
https://doi.org/10.1007/s40201-019-00435-1

RESEARCH ARTICLE

Microwave assist sorption of crystal violet and Congo red dyes onto amphoteric sorbent based on upcycled Sepia shells

K. Z. Elwakeel[1,2] · A. M. Elgarahy[3] · G. A. Elshoubaky[4] · S. H. Mohammad[3]

Received: 10 March 2019 / Accepted: 30 December 2019 / Published online: 15 January 2020

Abstract

A new sorbent based on Sepia shells (*cuttlefish bones*) has been synthesized (SSBC) and tested for the sorption of cationic dye (crystal violet, CV) and an anionic dye (congo red, CR). SSBC was produced by reaction of sepia shells powder with urea in the presence of formaldehyde. In the first part of the work, the sorbent was characterized using scanning electron microscopy, energy dispersive X-ray analysis, Fourier-transform infra-red spectrometry and titration (for determining pH_{PZC}). In a second step, sorption properties were tested on the two dyes through the study of pH effect, sorbent dosage, temperature and ionic strength; the sorption isotherms and uptake kinetics were analyzed at the optimum pH: Langmuir equation fits isotherm profiles while the kinetic profile can be described by the pseudo-second order rate equation. Maximum sorption capacities reach up to 0.536 mmol g^{-1} for CV and 0.359 mmol g^{-1} for CR, at pH 10.6 and 2.4, respectively. The comparison of sorption properties at different temperatures shows that the sorption is endothermic. Processing to the sorption under microwave irradiation (microwaved enforced sorption, MES) increases mass transfer and a contact time as low as 1 min is sufficient under optimized conditions (exposure time and power) reaching the equilibrium, while 2–3 h were necessary for "simple" sorption. Dye desorption was successfully tested using 0.5 M solutions of NaOH and HCl for the removal of CR and CV, respectively. The sorbent can be re-used for a minimum of four cycles of sorption/desorption. Finally, the sorbent was successfully tested on spiked tap water and real industrial wastewater.

Keywords Sepia shells functionalization · Sorption · Microwave enforced sorption · Sorbent recycling · Industrial wastewater

Introduction

The development of industry is strongly impacting the quality of water bodies. Uncontrolled discharge of domestic and industrial wastewaters into the environment is dramatically contaminating water resources [1]. Metallurgy, machinery, textile, printing, mining, rubber, paper and pharmaceutical industries are strong producers of contaminated water flows that may contain a great diversity of pollutants such as: dyes, heavy metals, phenols, pesticides, insecticide and drugs [2–8]. The presence of these pollutants in these water bodies above their allowable levels set by World Health Organization (WHO) and Environmental Agencies may have tremendous effects on human and animal health (neural toxicity, carcinogenicity, reproduction capabilities etc.), biotope quality (eutrophic effects, photosynthesis inhibition, etc.) due to poor degradability and/or highly accumulating effects [9–13].

Dye industry gives emblematic examples of the potential impact of uncontrolled management of contaminated flows. Dyes are used in a great diversity of sectors: textile, paper, leather, dyestuff, printing, plastic, cosmetics and coatings which are widely disseminated because of low cost production, brightness and high resistance against environmental conditions [14, 15]. Even at low concentration, dyes are optically active and detectable; their impact on water bodies is

Electronic supplementary material The online version of this article (https://doi.org/10.1007/s40201-019-00435-1) contains supplementary material, which is available to authorized users.

✉ K. Z. Elwakeel
Khalid_elwakeel@yahoo.com; Khalid_elwakeel@sci.psu.edu.eg

[1] Environmental Science Department, Faculty of Science, Port-Said University, Port-Said, Egypt

[2] University of Jeddah, College of Science, Department of Chemistry, Jeddah, Saudi Arabia

[3] Zoology Department, Faculty of Science, Port-Said University, Port-Said, Egypt

[4] Botany Department, Faculty of Science, Suez Canal University, Ismailia, Egypt

then very acute. Indeed, the dispersion of dyes in water assets disturbs gas solubility, which, in turn, affects the tills of aquatic organisms and disrupting their spawning sites and refuges. While hindering light penetration in water, the dyes also limits photosynthesis. Apart of these secondary effects, the dyes have frequently specific toxicity due to carcinogenic and mutagenic effects (associated to the presence of benzidines, and naphtalenes derivatives) [16–19].

Dyes can be classified into three categories: (a) anionic (acid, direct and reactive dyes) with negative charge mainly due to (SO_3^-) group, (b) cationic (basic dyes) due to protonated amine group and (c) nonionic (disperse dyes) according to their dissociation behavior in aqueous solutions [20]. Azo dyes either cationic or anionic bear one or more azoic bonds (N=N). Beside its stability against light, heat and aerobic digestion, it can cause acute diseases as genetic mutation, allergic problems, vomiting and cyanosis [21]. Crystal violet (CV) and Congo red (CR) dyes are two common examples of cationic and anionic dyes, respectively. They were chosen to be studied in this work as they are frequently used in a wide range of different industries. They have been also frequently investigated for testing sorbents; these two emblematic dyes have been also used in the present study for evaluating the sorption properties of the sorbent obtained by functionalization of sepia shells.

Congo red (CR) is the sodium salt of 3,3′-([1,1′-biphenyl]-4,4′-diyl)bis(4-aminonaphtalene-1-sulfonic acid); its chemical structure corresponds to [$C_{32}H_{22}N_6Na_2O_6S_2$] [22]. It is a benzidine-based anionic biazo dye, which is water soluble and yields a red colloidal solution. It is one of the most widely anionic dyes used in many field such as biology, biochemistry and textile industry [23]. It has many negative effects on human public health including vomiting, nausea, diarrhea, allergic problems and difficulty in breathing. In addition, it is easily metabolized to benzidine, which is identified as having possible carcinogenic effects for humans [24, 25]. Crystal violet (CV) (or gentian violet) is a triaminoarylmethane dye with the chemical structure [$C_{25}H_{30}N_3Cl$]. It is classified among the cationic dyes. It is extensively used in different industries such as pharmaceutical, paper, textile and printing ink [26, 27]. Despite its many medical benefits while using as a biological stain, a bacteriostatic agent in veterinary medicine and a skin disinfectant [28–30], it is harmful, depending on concentration, by different ways of exposure (inhalation, ingestion and skin contact). It is carcinogenic and can cause digestive tract, skin and eye irritation to human [31].

These harmful impacts of dyes clearly demonstrate that the removal of dyes from water bodies is an important issue for industry, environment and health. Numerous processes have been designed for the removal of hazardous dyes from aqueous media: coagulation/flocculation [32], photo oxidation [33], membrane separation [34], biological degradation [35–38], and irradiation [39]. Most of these methods have many drawbacks in their application, for example, high cost, production of toxic sludge, poor efficiency in low concentrations and in some cases the degradation of the dye may produce even more harmful sub-products. Consequently, exploring an efficient and straightforward route for dyes elimination remains a great challenge as a bottleneck for preserving water resources. Sorption and biosorption represent a promising alternative to conventional processes for reaching the levels of abatement of dye content endorsed by international or national regulations and the WHO [40, 41]. Biosorption consists of the use of materials of biological origin for sorbate binding according mechanisms similar to those use ion-exchange and complexation resins . It has many advantages such as simplicity, easy operation, low cost and high efficiency. Various sorbents like biochar [42], modified clay [43], chitosan [44], graphene [45], agriculture wastes [46–48], nanocomposites [49] and hydrogels [50] were used for dyes removal.

Sepia shells or cuttlefish bones (SS) are sub-products of fisheries. Despite being rich in calcium, they are usually disposed without any commercial valorization. This may cause locally some environmental nuisances; this is especially the case in the Port-Said area and using this by-product for application in dye removal would make a double benefit. A literature survey showed that very few work was performed on dye removal using cuttlefish bones [51, 52]. So the present work is focused on the use of this eco-friendly safe natural waste for assessing, after chemical modification, its capacity for dye removal. The sepia shells, collected from the fishing market of Port Said city (Egypt) and were chemically modified to prepare a new sorbent: sepia shells based composite (SSBC). The sorbent was physico-chemically characterized prior being tested for sorption of CR and CV from synthetic solutions: the effect of pH, temperature, ionic strength, and sorbent dosage were investigated before studying sorption isotherms and uptake kinetics. After testing dye desorption and sorbent recycling, the new sorbent was tested for the treatment for complex effluents (spiked tap water and real industrial effluent). The microwave irradiation strongly enhances uptake kinetics.

Materials and methods

Materials

Shells of *Sepia pharaonis*, urea, formaldehyde (solution 37% *w*/w) and acetic acid were supplied by Merck (Germany) as analytical grade reagents. All chemicals used were of analytical grade and distilled water was used for the preparation of all aqueous solutions. Congo red (CR) and Crystal violet (CV) dyes were supplied by Sigma-Aldrich (Switzerland). HCl (0.1–1.0 M) and NaOH (0.1–1.0 M) solutions were used to control pH of dye solutions.

Sepia shells powder (SS) preparation

Sepia shells (SS) were collected from fishing market, Port Said city, Egypt. Initially, they were washed three times with tap water to remove dirt and surface adhered particles. This is followed by rinsing in double-distilled water to remove any impurities until washing water became clear. They were dried naturally in the air for 4 days, followed by oven drying at 40 °C for 24 h until they reached constant weight. Pestle and mortar instruments were used for the shell powder preparation. Firstly, shells were smashed into small pieces by using pestle and then the obtained small pieces were further grinded using mortar. The product was finally sieved and stored in a desiccator until further use.

Synthesis of Sepia shells based composite (SSBC)

In order to enhance the removal efficiency of SS powder towards CV and CR dyes, the raw material was chemically modified to produce Sepia shells based composite (SSBC). Briefly, 15.2 g (0.2 mol) of urea were mixed with 40 mL of distilled water in a 250-mL two- necked flask equipped with a stirrer and condenser. The flask was heated until urea was dissolved. Then 15.2 g of the dried SS powder was added to the flask. Twenty five mL of formaldehyde (37% aqueous solution, containing 0.2 mol of formaldehyde) was added to the reaction mixture and the solution pH was adjusted to 3 with acetic acid. The reaction was carried out for 8 h under heating (95 °C) and stirring. The product was washed with dilute NaOH solution, distilled water, ethanol, and acetone. The product was sieved under open laboratory conditions using standard mesh (125 mm) sieve, dried in an oven at 100 °C for 4 h and stored in a polypropylene container in a desiccator.

Characterization of the sorbent

FT-IR of SSBC sorbent was examined in dried KBr powder by recording the infrared spectra over the range of 400–4000 cm^{-1} using a Fourier transform infrared (FTIR) spectrophotometer (FT/IR4100 Jasco-Japan).

The morphology of SSBC sorbent before and after binding to both CV and CR dyes was analyzed with Scanning Electron Microscope coupled with an Energy Dispersive X-ray analysis system (Jeol; JSM-6510LV). BET surface area, pore volume and pore size of SSBC sorbent was analyzed by Quantachrome NovaWin (Quantachrome Instruments).

The pH_{PZC} of the sorbent was determined using the pH-drift method. A fixed amount of the sorbent was mixed for 24 h with a given volume of 0.1 M NaCl (or Na_2SO_4) solution with initial pH (pH_i) varying between 1 and 10. The final pH (pH_f) was recorded and compared to initial value the pH_{PZC} corresponds to $pH_i = pH_f$.

Preparation of solutions

Stock single solutions (1000 mg L^{-1}) of CV and CR dyes were separately prepared in distilled water. The working solutions were obtained by dilution of the stock solutions with distilled water just before experiments. HCl (0.01–0.5 M) and NaOH (0.01–0.5 M) were used to change the acidity of the medium. CV and CR concentrations of all samples were analyzed by the spectrophotometry method at 590 and 497 nm, respectively, using photometer 7100, Palintest, USA.

Sorption experiments

To study the effect of solution pH, 20 mL of 20 mg L^{-1} of CV and CR solutions at different initial pH values (2.4–10.6) were individually blended with 0.03 g of SSBC sorbent for 90 min, and the stirring speed was maintained at 150 rpm using a reciprocal agitator, Rota bit, J.P. Selecta (Spain). PH values were adjusted by addition of 0.01–0.5 M HCl and 0.01–0.5 M NaOH solutions and measured by using a pH meter (Aqualytic AL15). Four mL of each test sample was withdrawn for centrifugation to avoid a risk of dyes sorption in case of cellulose filters usage for filtration purpose. The resultant supernatants were analyzed after centrifugation for residual CV and CR concentrations. The pH was not controlled during the sorption but the final pH was systematically recorded.

The effect of sorbent dose on CV and CR removal was performed by changing amount of SSBC sorbent from (0.01–0.1 g) mixed with 20 mL of dyes solutions separately (C_0: 20 mg L^{-1}) at 25 ± 1 °C for 90 min.

For sorption isotherms, 0.03 g of SSBC sorbent was separately mixed with 20 mL of CV and CR solutions at different initial concentrations (C_0, ranging between 10 and 1000 mg L^{-1}) at 150 rpm for 90 min. After solid/liquid separation, the residual concentrations of CV and CR were determined. Sorption capacity (q_e, mmol g^{-1}) and removal % were determined by the following mass balance equations, respectively:

$$q_{eq} = \frac{(C_0 - C_e)V}{m} \quad (1)$$

$$\%\text{Removal} = \frac{C_0 - C_e}{C_0} \times 100 \quad (2)$$

Where C_0 and C_e is the initial and equilibrium concentration of dye in solution (M), respectively, V is the volume of solution (L) and m the mass of sorbent (g).

Langmuir [53], Freundlich [54], Dubinin−Radushkevich (DR) [55], and Temkin [56] sorption isotherm are applied to clearly explain both CV and CR dyes sorption equilibrium data on SSBC composite. Different important data related to the aforementioned mathematical models could be derived

from experimental points. The mentioned isotherm models are displayed in the Table S2 (see Supplementary Information).

The dimensionless constant separation factor, R_L, is essential characteristics of Langmuir isotherm model and can be calculated using the following equations:

$$R_L = \frac{1}{1 + K_L C_0} \quad (3)$$

Where K_L is the Langmuir equilibrium constant and C_0 is the initial concentration of dye. Values of $0 < R_L < 1$ indicates the suitability of the process.

Another important parameter is the mean energy of sorption (E_a, kJ mol^{-1}) which can be calculated by applying Dubinin and Radushkevich isotherm model equation. Generally the value of (E_a) is the limit energy for distinguishing between physical and chemical sorption. If it lies below 8 kJ mol^{-1}, this means physical sorption, while in range (8–16) kJ mol^{-1} is ion exchange and above 16 kJ mol^{-1} indicates chemical sorption. It can be denoted from the following equations:

$$\varepsilon = RT \ln\left(1 + \frac{1}{C_{eq}}\right) \quad (4)$$

$$E_a = \frac{1}{(2K_{DR})^{0.5}} \quad (5)$$

Where ε is the Polanyi potential, R is the universal gas constant (8.314 J mol^{-1} K^{-1}) and T is the absolute temperature (K).

For sorption kinetics, 0.3 g of SSBC sorbent was separately placed in contact with 200 mL of CV and CR solutions for 180 min (C_0: 20 mg L^{-1}). Samples (5 mL) were collected at fixed times and the residual concentrations were determined. The agitation speed was set at 150 rpm while the temperature was maintained at 25 ± 1 °C. The sorbed amount of CV and CR per unit weight of the sorbent at time t (q(t), mmol g^{-1}) was calculated from the following mass balance equation (taking into account the decrement in the volume of the solution).

$$q(t) = \sum_{i=1}^{n} \frac{\left(C(t)_{(i-1)} - C(t)_{(i)}\right) \times V(t)_{(i-1)}}{m} \quad (6)$$

where $C(t)_{(i)}$ (M) is the CV and CR concentrations of the withdrawn sample number i at time t. $C(t)_{(0)} = C_0$, $V(t)_{(i)}$ (mL) is the volume of the solution in the flask at sample number i and time t, and m is the mass of the sorbent in the flask. The sample volume $V(t)_{(i)}$-$V(t)_{(i-1)}$ equals 5 mL. An error analysis (sum of squared errors of prediction; SSE) was also established to compare the validity of kinetic and isotherm models using the following equation:

$$SSE = \sum_{n=1}^{n} \left(q_{cal} - q_{exp}\right)^2 \quad (7)$$

Where q_{cal} and q_{exp} are the calculated and experimental adsorption capacities.

In order to analyze sorption kinetics of both CV and CR dyes on SSBC sorbent, simple models based on different theoretical foundations were used, including pseudo first order (PFORE) [57], pseudo second order (PSORE) [58], Weber and Morris model [59] and Elovich model [60] are applied to model the obtained experimental data and therefore facilitate interpretation of process. The models equations forms are reported in Table S3 (see Supplementary Information).

The influence of temperature on the sorption of CV and CR was carried out by mixing 20 mL of both dyes solutions (C_0: 20 mg L^{-1}) individually with 0.03 g of SSBC sorbent for 90 min at various temperatures (298, 308, 318 and 328 K). Thermodynamic parameters such as Gibbs free energy change (ΔG^o), standard enthalpy change (ΔH^o) and standard entropy change (ΔS^o) are used to interpret the sorption thermodynamic through providing information about spontaneity, feasibility and nature of sorption process whether it is exothermic or endothermic reaction. They can be estimated as follow:

$$K_c = \frac{C_S}{C_e} \quad (8)$$

where K_c is equilibrium constant. C_s and C_e are equilibrium concentrations of sorbate onto the sorbent surface and in aqueous solution, respectively.

Classic van't Hoff reaction isotherm equation correlates between free energy change (ΔG), standard free energy change (ΔG^o) and equilibrium constant (K_c) at constant temperature (T) as:

$$\Delta G = \Delta G^o + RT \ln K_c \quad (9)$$

At equilibrium, ΔG = zero; hence Eq. 9 is reduced as follow:

$$\Delta G^o = -RT \ln K_c \quad (10)$$

This is the most important equation used in sorption thermodynamics to predict the feasibility of sorption process. To predict ΔH^o and ΔS^o, Eq. 10 rearranged in the form of:

$$\ln K_c = \frac{\Delta G^\circ}{-RT} \quad (11)$$

ΔG^o is also related to ΔH^o and ΔS^o at constant temperature by the following equation:

$$\Delta G^o = \Delta H^o - T\Delta S^o \quad (12)$$

Therefore van't Hoff equation becomes:

$$\ln K_c = \frac{-\Delta H^\circ}{RT} + \frac{\Delta S^\circ}{R} \quad (13)$$

Effect of ionic strength on CV and CR sorption was examined by addition of ascending concentrations of NaCl from 5 to 45 g L^{-1} to 20 mL CV and CR solutions for 90 min (C_0: 20 mg L^{-1}, sorbent dosage: 0.03 g).

The methodology relied on potential implementation of microwave-enforced sorption (MES) technique was evaluated by using microwave apparatus which is a household oven (CLATRONIC MWG 756 E) model operates with rated power output of 800 watt, frequency of 2.45 GHz and cavity volume of 20 L. Preliminary experiment related to individual effect of microwave radiation on both CV and CR degradation reaction in the absence of SSBC composite was performed. It was carried out by introducing 20 mL of both dyes solutions (C_0: 20 mg L^{-1}) separately to microwave radiation without addition of SSBC sorbent at adjusted varied time interval (5, 10, 15, 20, 25, 30, 35, 40, 45, 50, 55 and 60 s) at 800 watt. The degradation efficiency (%) of dye can be determined through the following equation:

$$\text{Degradation efficiency } (\%) = \frac{(C_o - C_e)}{C_o} \times 100 \qquad (14)$$

Where C_o and C_e are the initial and final concentrations of the studied dye.

MES technique feasibility was appraised through two key factors; microwave radiation time and microwave power intensity. Studying effect of microwave radiation time is very necessary to evaluate the influence of radiation exposure time on sorption process. Microwave heating time was examined by mixing of 0.03 g of SSBC sorbent with 20 mL of CV and CR single solutions (C_0: 20 mg L^{-1}) at different time intervals (5, 10, 15, 20, 25, 30, 35, 40, 45, 50, 55 and 60 s). The microwave power is one of the main parameters influencing on the sorption capacity yield. For microwave power intensity experiment, 0.03 g of SSBC sorbent was separately mixed with 20 mL of CV or CR solutions (C_0: 20 mg L^{-1}) at different microwave power intensities (ranging from 144 to 800 watt) for only 1 min to avoid water evaporation. Two aforementioned tests related to microwave radiation effect were carried out with maximum exposure time of 1 min to avoid boiling of the solution.

Reusability studies were executed after completion of sorption process by separately contacting 0.03 g of SSBC composite with 20 mL of CV and CR solutions (C_0: 100 mg L^{-1}) at 25 ± 1 °C for 90 min. Sorption capacity and removal efficiency were determined by using two equations (Eq. 1, 2) respectively. The loaded sorbent was collected from two dyes solutions by centrifugation and washed by distilled water. Then it was separately mixed with 10 mL of 0.5 M of HCl and 0.5 M of NaOH at 25 ± 1 °C for 30 min in order to desorb CV and CR, respectively. The regenerated sorbent was carefully washed by distilled water for reuse in the next cycle. The procedure was repeated for 4 cycles. Regeneration efficiency (RE, %) was calculated according to the following equation:

$$\text{RE}\% = \frac{Amount\ of\ dye\ sorbed\ \ (mmol) at\ run\ (n+1)}{Amount\ of\ dye\ sorbed\ \ (mmol) at\ run(1)} \times 100 \qquad (15)$$

Where n is the number of regeneration cycle.

All experiments were always performed thrice. The limit of experimental errors of triplicates was ±5%.

Test of dyes sorption capacity from complex solutions

Applicability of SSBC sorbent to be used as color removing material for CV and CR dyes from two real water samples was evaluated. The first sample was tap water and the second was wastewater collected from petrochemical plant discharge, Port Said, Egypt. Eight different concentrations of CV and CR (5, 10, 15, and 20 mg L^{-1}) were spiked into the selected water samples from the two mentioned sources. A mass of 0.03 g of SSBC sorbent was individually mixed with 20 mL of CV and CR samples at different concentrations, 150 rpm for 90 min. The samples were centrifuged and supernatants were analyzed for residual CV and CR concentrations.

Results and discussions

Sorbent characterization

A detailed characterization of the sorbent was already published [61]. Complementary information is presented in the supplementary Material Section (Section I).

Cationic and anionic dyes sorption properties

Influence of pH

Influence of solution pH on sorption process is a critical parameter to be studied as it simultaneously effects on the surface charge of the sorbent in addition to the ionization degree and chemical structure of organic dyes under study. So the effect of pH was examined by varying initial pH of dyes solutions in the range between 2.4–10.6 and observing its effect followed by detecting the optimum pH values at which sorbent reached to maximum grade for dyes removal percentages (Fig. 1). The removal efficiency of SSBC is depended on the solution pH and chemical ionization of the studied dyes. For the sorption of CV dye (cationic dye), it can be noted that the uptake value was 0.022 mmol g^{-1} at pH_i = 2.4 (the removal (%) = 66.5%). Then it elevated with increasing pH reaching

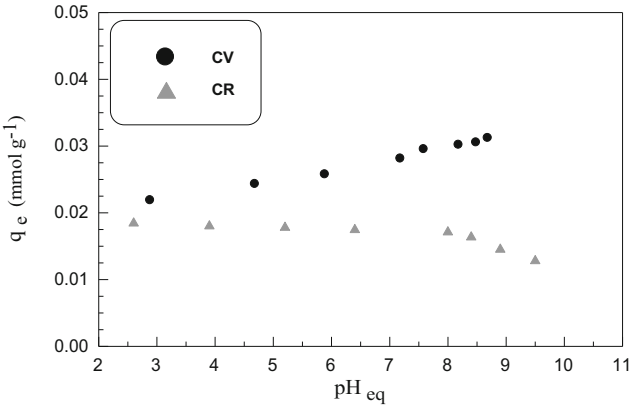

Fig. 1 pH effect on CV and CR dyes sorption onto SSBC; (T: 25 ± 1 °C; C_0: 20 mg L^{-1}; sorbent mass 1.5 g L^{-1})

to 0.031 mmol g^{-1} equal (the removal (%) = 95.05%) at pH_i = 10.6. Contrarily, in case of anionic dye, CR, a quite opposite sorption behavior was noticed. It can be noted that the highest uptake value was 0.019 mmol g^{-1} (the removal (%) = 97.4%) at pH_i = 2.4 then decreased to 0.013 mmol g^{-1} nearly (the removal (%) = 67.9%) at pH_i = 10.6. Figure 2 shows that the point of zero charge (pH_{PZC}) for SSBC was at pH 7.6 which means that below it, the sorbent surface is positively charged while above it, sorbent surface is negatively charged. As cationic dye, CV, is positively charged, its sorption on SSBC surface was lower in acidic region due to electrostatic repelling forces and competition between H^+ and CV^+ to be adsorbed on SSBC surface. Whilst elevation of sorption in basic region is related to electrostatic attraction forces between negatively charged sorbent surface and positively charged dye molecules [62–64]. In the alkaline medium, addition of base leads to the presence of more OH^- ions and consequently deprotonation of $–NH_3^+$ on the sorbent surface and hence sorbent possess negative charge. On the contrary, as anionic dye, CR, is negatively charged, its sorption on SSBC sorbent was favorable in acidic medium because of electrostatic attraction forces between protonated amino groups on sorbent

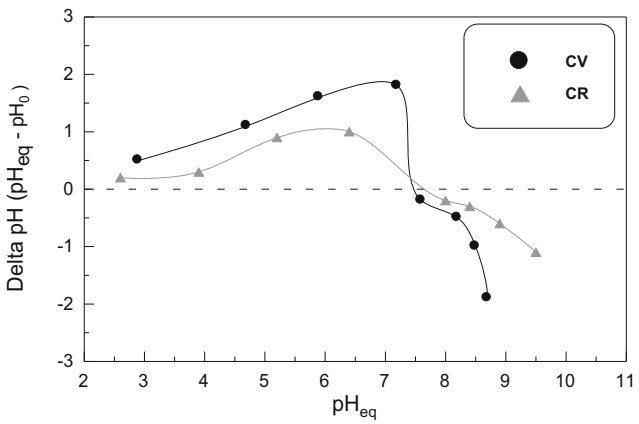

Fig. 2 Graph of ΔpH ($pH_{eq} – pH_0$) against initial pH (pH_0) from CV and CR sorption

surface with sulphonate (SO_3^-) groups from dye molecules. The reduction of CR sorption in basic medium due to electrostatic repulsion forces as well as competition between OH^- and CR^- to be sorbed on SSBC surface. Moreover the HSO_3^- in CR molecule will convert into $–SO_3Na^+$ radical which will dilute negative charge of CR and increase OH^- concentration [65–67]. In general, it can be noted that the lowest removal % values for CV and CR dyes in unfavorable conditions were 66.5% and 67.9%, respectively. This reflects the high aptitude of SSBC sorbent to be applied as substitute adsorbent for different organic dyes in a wide range of pH values.

Effect of sorbent dosage (SD)

The effect of sorbent dose (SD) on both CV and CR dyes sorption was investigated by changing solid to liquid ratio as sorption efficiency mainly depends on surface area and availability of more binding sites on sorbent surface. Equilibrium sorption capacities of SSBC exhibit a significant decline (about 9 times from 0.086 mmol g^{-1} to 0.009 mmol g^{-1} and from 0.051 mmol g^{-1} to 0.005 mmol g^{-1} for CV and CR, respectively) (Fig. S4(a), see Supplementary Material). While Fig. S4(b) (see Supplementary Material) display an increase in the removal % from 87.85% to 94% and from 89.9% to 95.85% for CV and CR, respectively, with increasing SSBC dosage from 0.5 to 5 g L^{-1}. It is evident that by introducing more amount of sorbent, the removal % enhanced due to increasing of overall surface area. Alternatively, more active sites became available for binding with dyes molecules [68]. Meanwhile with further increasing of sorbent dose, constant or slightly reduction of removal % was observed. This may be interpreted due to the blocking of some sorption sites via partial aggregation or overlapping of sorbent particles at high sorbent doses (known as screen effect on sorbent surface). This phenomenon resulted from unsaturation of vacant sites on sorbent surface due to constant concentration of dyes molecules compared with high amount of sorbent. It is known that dyes molecules can be sorbed by only a certain number of active sites, so any additional increase in the amount of sorbent will not be useful for total dye molecules sorption [69].

Sorption kinetic

Sorption kinetic is a very crucial factor for providing full knowledge about sorption dynamic and its rate controlling step. It is one of the basic requirements in modeling any industrial application. As shown in Fig. 3a, b, the sorption capacities of SBCC towards CV and CR dyes rapidly increased in the initial phase. This obviously appeared through the high removal % of both dyes that exceeded 90% after only 10 min, then sorption rate for both dyes gradually slow down till reaching equilibrium after 180 min. The very fast sorption rate in the initial stage can be attributed to great number of free

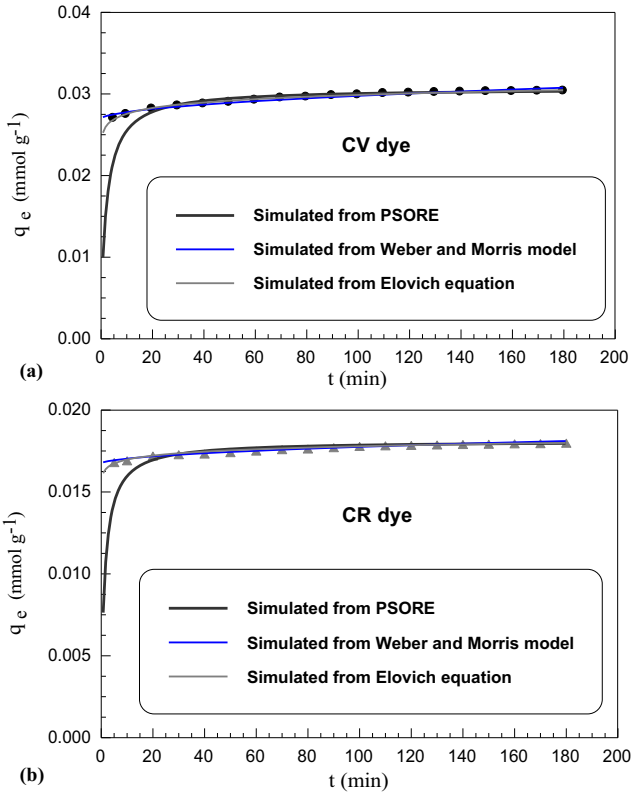

Fig. 3 Uptake kinetics of (a) CV dye (b) CR dye sorption onto SSBC (C_0: 20 mg L^{-1}; T: 25 ± 1 °C; volume: 200 mL; sorbent mass 0.3 g) at normal sorption

Table 1 Kinetic parameters of CV and CR sorption

Kinetic models	Parameter	CV	CR
PFORE	$k_1(min^{-1})$	0.026	0.0207
	q_e (mmol g^{-1})	0.0046	0.0015
	R^2	0.966	0.980
	SSE	0.013	0.005
PSORE	k_2 (g $mmol^{-1}$ min^{-1})	15.60	40.10
	q_e (mmol g^{-1})	0.0306	0.0180
	R^2	0.999	0.999
	SSE	3.46×10^{-5}	8.24×10^{-06}
Intraparticle diffusion	K_i ($mmolg^{-1}$ $min^{0.5}$)	0.0003	0.0001
	X (mmol g^{-1})	0.0268	0.0167
	R^2	0.954	0.975
	SSE	8.27×10^{-07}	5.71×10^{-08}
Elovich equation	α (mmol g^{-1} min^{-1})	7.31×10^{7}	1.52×10^{16}
	β (g $mmol^{-1}$)	994.07	2806.55
	R^2	0.992	0.978
	SSE	1.43×10^{-07}	4.98×10^{-08}

sorption sites available on sorbent surface that could be easily occupied by dyes molecules due to high concentration gradient between sorbent and dyes molecules. It is then followed by a slower rate reaching to a plateau condition "equilibrium phase". The saturation of sorbent active sites with dyes molecules leads to difficulty of unsaturated sites to be accessed with dyes molecules as a result of repulsion forces between the dyes molecules sorbed on the sorbent surface and in bulk phase [70].

As batch technique is customarily used as a preliminary step to evaluate sorbent efficiency for removing pollutants from their matrices, so effect of different assistant methodologies was tested. Heating is one of the most assisted factors to sorption because it can provide solute with adequate energy required for its migration from its medium to sorbent surface. Among the traditional heating methods, microwave radiation as a novel technique and high energy input source represents a promising and fast approach for reduction of sorption equilibrium time [71]. It is a superfast methodology used in different synthesis, separation and extraction process through intensifying the rate of chemical reaction on multi-fold [72–75]. Table 1 illustrated the sorption kinetics data of both dyes onto SSBC sorbent. While Table 2 reports the influence of microwave radiation on these kinetic parameters. As shown in Fig. 4a, b, the increase of SSBC uptake values (mmol g^{-1}) as well as the very fast sorption rate of the studied dyes upon increasing the microwave heating time can be explained by the effect of microwave radiation which accelerate and enforce solute molecules to migrate from solution matrix to sorbent surface and thus being sorbed on sorbent surface in a short period [76]. As a result of interaction between microwave radiation and bulk of aqueous medium through photocatalytic reaction assisted with microwave irradiation, the orientation of molecules changes and simultaneously increases the dipolar rotations of the polar groups molecules found in aqueous medium. Finally it leads to generation significant amount of heat occurs [77]. Different forms of heat including thermal, specific excitation and non-thermal effects are produced as outputs of microwave radiation usage. The thermal and specific excitations are effective for different pollutants degradation through contribution of hydroxyl radicals which are formed and being very effective in contaminants degradation [77]. The non-thermal energy also plays an important role by increase vibrational and rotational levels of molecules, therefore saturation time are shortened to only few seconds. Similar findings were obtained by other [76–78]. As any sorption process can be described as a mass transfer process, the microwave radiation represents a sustainable and superfast technique because it characterizes by attaining high operation performance in only few seconds compared with normal sorption case [79–81].

Assumption of pseudo first order (PFORE) is built on that rate change of solute ion removal with time is directly proportional to the difference in saturation concentrations [82], while pseudo second order (PSORE) is usually associated with the

Table 2 Kinetic parameters of the microwave enforced sorption of CV and CR

Kinetic models	Parameter	CV	CR
PFORE	$k_1(min^{-1})$	4.072	2.92
	q_e (mmol g^{-1})	0.0058	0.0020
	R^2	0.935	0.947
	SSE	0.007	0.003
PSORE	k_2 (g $mmol^{-1}$ min^{-1})	1616.78	3711.60
	q_e (mmol g^{-1})	0.0313	0.0184
	R^2	0.999	0.999
	SSE	4.52×10^{-06}	1.47×10^{-06}
Intraparticle diffusion	K_i (mmol g^{-1} $min^{0.5}$)	0.0046	0.0019
	X (mmol g^{-1})	0.0265	0.0164
	R^2	0.960	0.970
	SSE	4.9×10^{-07}	6.17×10^{-08}
Elovich equation	α (mmol g^{-1} min^{-1})	5.0×10^{06}	4.35×10^{10}
	β (g $mmol^{-1}$)	713.40	1759.48
	R^2	0.995	0.978
	SSE	6.00×10^{-08}	4.64×10^{-08}

situation when the rate of direct sorption/desorption process controls the overall sorption kinetics [83]. The agreement between experimental data and applied models was checked by determination coefficient (R^2) as well as sum of squared errors

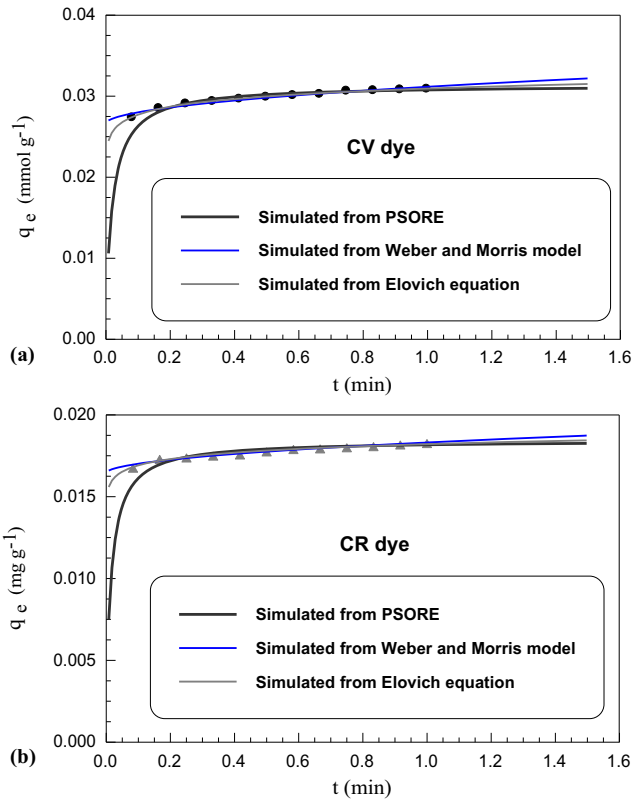

Fig. 4 Uptake kinetics of (a) CV dye (b) CR dye sorption onto SSBC (C_0: 20 mg L^{-1}; T: 25 ± 1 °C; volume: 20 mL; sorbent mass 0.03 g) at microwave enforced sorption

of prediction (SSE) to evaluate the best models describes CV and CR sorption on SSBC sorbent. By comparing the calculated R^2 and SSE of the two dyes sorption, it can be noted that the best coefficients of determination and the smallest SSE value agreed with the PSORE for both normal sorption (NS) and microwave enforced sorption (MES). This reflected the involvement of chemical reaction during sorption process.

Utilization of intraparticle diffusion and Elovich models paves away for more attesting about sorption mechanism and its rate controlling step. In any solid-liquid sorption system, mass transport can be ascribed by three consecutive steps: i) external mass transfer from bulk solution to sorbent surface, ii) inward diffusion stage and iii) adsorption onto sorbent surface binding site [84]. The plots of experimental data of dyes sorption at NS and MES (Fig. S7, see Supplementary Material) show that linear plots didn't pass through the origin for both dyes suggesting that sorption involved intraparticle diffusion but it isn't the rate controlling step may be other effects such as a boundary layer effect [85]. However, X parameter gives an idea about the thickness of the boundary layer surrounding sorbent surface [86]. X values were 0.0268, 0.0167 at NS and 0.0265, 0.0164 (mmol g^{-1}) at MES for CV and CR, respectively. This clearly shows the influence of microwave radiation on minimizing of the boundary layer effect through sorption process.

Finally, the kinetic model proposed by Elovich was applied. The Elovich equation assumes that the sorbent active sites are heterogeneous and therefore possess different sorption energies [87]. The parameters obtained from Elovich equation a long with the corresponding R^2 and SSE are reported in Tables 1 and 2 for NS and ME, respectively. The values of α and β related to both dyes sorption were

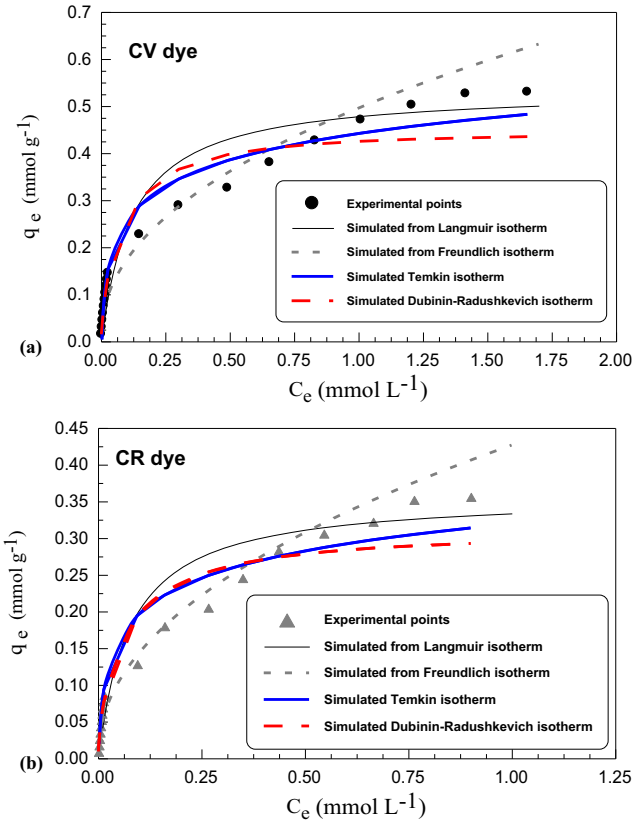

Fig. 5 Effect of dyes concentrations on the sorption process for (a) CV dye, (b) CR dye, (sorption time 90 min, sorbent dosage 1.5 g L^{-1} and at 20 °C)

determined from the intercept and slope, respectively, of the linear plot of q_t against ln*t*. The values of α which represents initial sorption rate were 7.31×10^{7}, 1.52×10^{16} (mmol g^{-1} min^{-1}) for NS and 5.0×10^{06}, 4.35×10^{10} (mmol g^{-1} min^{-1}) for MES for CV and CR dyes, respectively. This reflects the availability of many binding sites on SSBC surface for fast occupation by both CV and CR dyes molecules.

By applying the studied kinetics models on the microwave assist sorption process, it was found that sorption kinetic behavior of both CV and CR on SSBC sorbent at MES follow the same behavior of kinetic models at NS. As reported in Table 2, the MES sorption of both CV and CR dyes on SSBC sorbent showed the highest R^2 and lowest SSE in case of PSORE. The values of k_2 increased from 15.60, 40.10 to 1616.78, 3711.60 g $mmol^{-1}$ min^{-1} for CV and CR dyes, respectively. This clarify that microwave radiation significantly increased the sorption rate.

Degradation reaction of CV and CR dyes under microwave radiation

The comparison between both CV and CR dyes degradation rates and removal efficiencies under individual microwave radiation and in the presence of SSBC composite is very important to determine the sorption characteristics of SSBC accurately. Generally, degradation efficiency % can be detected by observing the difference between initial and final dyes concentrations before and after being exposed to microwave radiation respectively. Highest percents for dyes degradation under microwave radiation were 5.15% and 5.5% after 1 min for CV and CR dyes, respectively. Extent of dyes degradation

Table 3 Isothermal parameters of CV and CR sorption

Isothermal models	Parameter	CV	CR
Langmuir	K_L(L $mmol^{-1}$)	8.24	13.03
	q_m (mmol g^{-1})	0.536	0.359
	R^2	0.975	0.965
	SSE	0.042	0.022
Freundlich	n	2.18	2.11
	K_f (mmol g^{-1}) (L $mmol^{-1})^{1/n}$	0.495	0.426
	R^2	0.940	0.947
	SSE	0.023	0.007
Temkin	A (L g^{-1})	0.2355	0.4038
	B (kJ mol^{-1})	30.456	46.2807
	R^2	0.9587	0.9401
	SSE	4.32×10^{-02}	1.94×10^{-02}
Dubinin-Radushkevich	q_{DR} (mmol g^{-1})	0.443	0.305
	K_{DR} (J^2 mol^{-2})	1.49×10^{-8}	1.24×10^{-8}
	E_a (kJ mol^{-1})	5.80	6.34
	R^2	0.984	0.981
	SSE	0.026	0.017

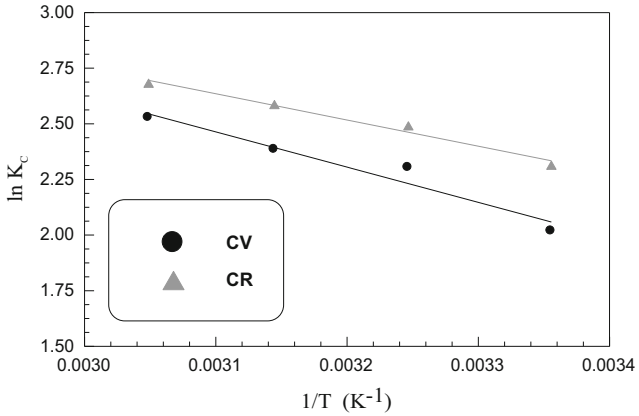

Fig. 6 van't Hoff plots for CV and CR dyes sorption

depends mainly on the interaction between formed hydroxyl radicals and target dyes molecules. While the removal efficiencies of SSBC towards CV and CR dyes were 93.7% and 95.5%, respectively. The obtained results revealed the superior ability of SSBC to sequester both CV and CR dyes from water system under microwave radiation. Similar results were recorded by other [88, 89].

Sorption isotherm

Sorption isotherm is essential to be studied through different mathematical models. This is to obtain basic information that accurately describes sorbent – sorbate interaction and the subsequent utilization for design and optimization purpose [90].The rate of both CV and CR sorption on SSBC sorbent increased with increase of initial dyes concentration. This may be attributed to the concentration gradient acting as a driving force that accelerates sorption process to achieve the equilibrium stage. Different sorption isotherm models: Langmuir, Freundlich, Dubinin−Radushkevich (DR) and Temkin are implemented to clarify both CV and CR dyes sorption equilibrium data and hence determining their sorption capacities (Fig. 5). Parameters that derived from these isotherm models are shown in Table 3. Langmuir isotherm model assumes that sorption takes place at the specific homogeneous sites within the sorbent. Once a sorbate molecule occupies a site, no further sorption can take place meaning monolayer sorption. Also, all sorption sites are identical and energetically equivalent [91]. While Freundlich isotherm model based on the assumption of a heterogeneous distribution of the sorption sites (basically corresponding to different affinities of sorbent to sorbate) as well as possible multilayer accumulation [92]. A comparison of R^2 and SSE calculated from the experimental values (Figs. S9, Supplementary Information) of the previous models related to two dyes sorption was tabulated in Table 3. Sorption data of both CV and CR dyes on SSBC sorbent promotes better agreement with Langmuir model than Freundlich model through highest R^2 and lowest SSE values derived from experimental data.

In the present study, R_L values of SSBC that calculated from Eq. 3 lie between 0.05 and 0.98 for all concentrations of CV and CR dyes at 25 °C. These values are less than 1.0, therefore the sorption is very favorable whatever the concentrations range.

Temkin's isotherm based on hypothesis that decline in the heat of sorption of all molecules is linear, rather than logarithmic with coverage (Fig. S9 (c), see Supplementary Information) [93]. The Temkin constant B values were 30.45 and 46.28 kJ mol^{-1} for CV and CR, respectively, these values refer to the physical nature of the sorption process.

Dubinin and Radushkevich (D-R) isotherm was developed, taking into account the effect of the porous structure of the sorbent, and the energy involved in the sorption process. The slop of plot of ln q_{eq} vs.ε^2 (Fig. S9 (d), see Supplementary Information) gives K_{DR} and the intercept yields Q_{DR}. The D–R constant (K_{DR}) derived from Eq. 5 can give valuable information regarding the mean energy of sorption (Ea, kJ mol^{-1}). The results of D–R isotherm for both dyes are reported in Table 3. Their values are 5.801 and 6.342 kJ mol^{-1} for CV and CR, respectively. This is in consistent with the proposed mechanism of physical sorption.

Influence of temperature

Studying influence of temperature change on sorption process is very important for getting insights about its nature. It was observed that the increase in sorption capacity of SSBC was in direct proportion to the increase in temperature. This can be explained by the decline in solution viscosity with raising temperature. This leads to increase in dyes molecules mobility

Table 4 Thermodynamic parameters of CV and CR sorption

Dye	ΔH^o (kJ mol^{-1})	ΔS^o (kJ mol^{-1} K^{-1})	R^2	$T\Delta S^o$ (kJ mol^{-1})				ΔG^o (kJ mol^{-1})			
				298 K	308 K	318 K	328 K	298 K	308 K	318 K	328 K
CV	13.17	0.061	0.948	18.27	18.88	19.50	20.11	−5.10	−5.71	−6.33	−6.94
CR	9.81	0.052	0.981	15.59	16.12	16.64	17.16	−5.78	−6.30	−6.83	−7.35

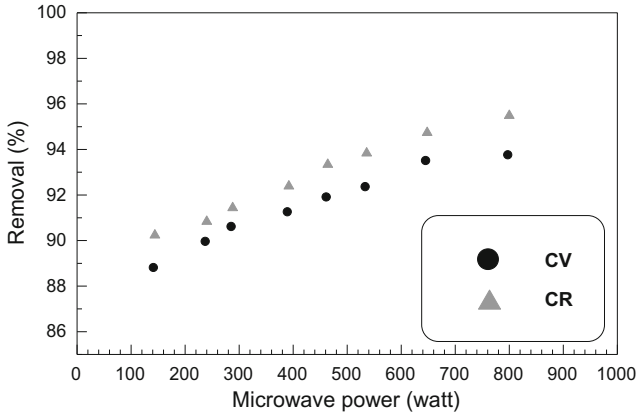

Fig. 7 Effect of different microwave power intensities on CV and CR removal % (C_0: 20 mg L^{-1}; T: 25 ± 1 °C; volume; 20 mL; sorbent mass: 0.03 g)

followed by their feasible penetration through sorbent pores, reaching to available sorbent active sites and hence increase in chemical interaction between sorbate molecules and different active sites on sorbent surface [94]. The values of ΔH^o, ΔS^o, ΔG^o and $T\Delta S^o$ for the sorption of both CV and CR dyes on SSBC sorbent are determined from the linear plot of lnK versus 1/T according to Eq. 13 (Fig. 6) and reported in Table 4. The calculated free Gibbs energy change values from CV and CR sorption suggest the spontaneous nature of both sorption processes. The decline in ΔG^o values with temperature elevation for both dyes sorption affirms the increase in spontaneity degree as well as the favourability of the process at high temperature [95]. As literature reports that if values of ΔG^o lie in the range − 20 to 0 kJ/mol, means physical sorption and in between −400 and − 80 kJ mol^{-1} indicates chemical sorption [96]. Accordingly, based on the obtained results from the present study, sorption process of both dyes may be physisorption. Both enthalpy change ΔH^o and entropy change ΔS^o values for two dyes sorption were calculated from slope and intercept of the linear plot of Eq. (13) and listed in Table 4. This table also elucidate that the positive values of ΔH^o for both dyes confirm the endothermic nature of sorption process. Besides, the positive ΔS^o values for both dyes indicate increase in randomness at the solid/liquid interface during sorption process [97].

Effect of microwave power on sorption (MES)

Evaluation the influence of different microwave power intensities on sorption process behavior is very necessary. It was observed that there is a direct relationship between sorbent removal % and microwave power intensity. As microwave power intensity increased from 144 to 800 watt, the sorbent removal % increased in only 1 min from 88.75% to 93.7% and from 90.3% to 95.55% for CV and CR respectively (Fig. 7). The obtained results depicted the positive effect of augmentation of microwave power intensity on raising removal % of SSBC against both dyes. The enhancement of SSBC sorption capacities towards both CV and CR can be ascribed by sorbent structure expansion and enlargement of sorbent surface area with the formation of new pores. This may be due to the combination effect of internal and volumetric heating that triggered dyes molecules migration rate from solution to the sorbent surface [98]. This is in agreement with endothermic nature of the sorption behavior. Although raising microwave power nearly 5 fold, slight increase in SSBC sorption capacities was achieved. This was endorsed with similar findings about the implementation of microwave technique during some extraction process [99, 100].

Effect of ionic strength

Consumption of several salts in the dying process with different concentrations depending mainly on the source and type of the industrial effluents. So, competitive sorption study is necessary to infer the effect of interfering ions coexistence on the ability of SSBC to sorb CV and CR dyes as natural water and wastewaters containing different elements in their solutions. The presence of these elements may lead to interaction or competition between them from hand and dyes molecules from the other hand for being sorbed on sorbent active sites. This may inhibit or raise removal % of sorbent toward both CV and CR dyes. So, SSBC sorbent efficiency was tested by adding ascending concentrations of NaCl. It was observed that sorption

Table 5 Sorption, Removal (%) and regeneration efficiency (RE, %) of CV and CR

Sorption/ desorption cycle	(CV)			(CR)		
	Amount sorbet (mmol g^{-1})	Removal (%)	RE (%)	Amount sorbet (mmol g^{-1})	Removal (%)	RE (%)
First sorption operation	0.147	90	–	0.088	91.68	–
Cycle 1	0.145	88.88	98.75	0.087	90.72	98.95
Cycle 2	0.144	88.19	97.98	0.087	90.21	98.39
Cycle 3	0.143	87.75	97.50	0.086	89.85	98.00
Cycle 4	0.142	87.22	96.91	0.086	89.55	97.67

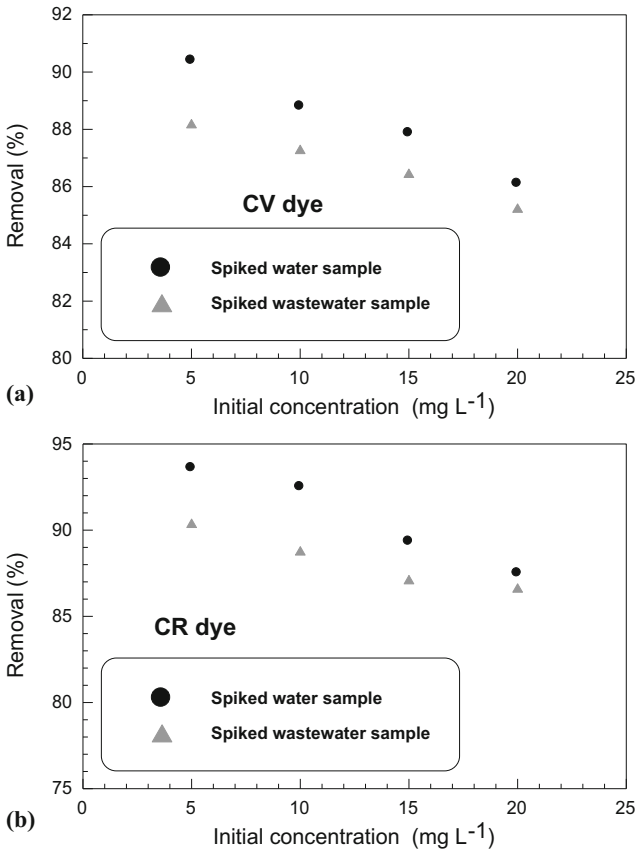

Fig. 8 Removal (%) of SSBC towards CV and CR dyes from different concentrations of spiked water samples for (a) CV dye, (b) CR dye, (sorption time 90 min, sorbent dosage 1.5 g L^{-1} and at 20 °C)

capacities of SSBC declined from 0.029 to 0.022 mmol g^{-1} and from 0.017 to 0.013 mmol g^{-1} for CV and CR, respectively, with increasing initial concentrations of NaCl from 5 g L^{-1} to 45 g L^{-1} (Fig. S10, Supplementary Information).This may be due to the shield effect or "salting out effect" phenomena as a result of the presence of NaCl. This may influence on the interaction between solid sorbent surface and dye molecules and lead to decline in the adsorbed dyes molecules [94]. Another reason for the decline in removal % of SSBC in high NaCl concentrations may be due to the probability of increasing ionic strength that effect on the activity coefficient of dyes and sorbent active sites. In addition to the competition effects between Na^+ and Cl^- ions against CV^+ and CR^- respectively [101].

Reusability study

The ability of exhausted sorbent to be regenerated and then reused is very crucial from both economic and ecological aspects. It determines the feasibility of sorbent for using in repeated cycles. Based on the results, its potential to be used in large scale will be supported, becoming a green, superior and alternative approach for traditional scenarios for dyes removal [102]. Selected desorbing agents should be available, effective, safe and low cost. Two different medium were used in order to maximize desorption of opposite charged dyes from SSBC surface. Both HCl and NaOH can be used as effective desorbing agents for CV and CR, respectively. Table 5 shows sorption, removal % and regeneration efficiency (RE, %) for CV and CR dyes. When SSBC was saturated with CV, its immersion in acidic medium by using 0.5 M HCl promoted CV dye molecules desorption and it's RE, % decreased from 98.75% to 96.91% in the fourth cycle. While, in case of SSBC saturation with CR dye molecules, it's RE, % declined from 98.95% to 97.67% in the fourth cycle, by using 0.5 M NaOH. Our results elucidated that in the first cycle, SSBC composite sorbed above 60 mg g^{-1} of both CV and CR dyes, i.e. about 27% its sorption capacity (Qmax>218 mg g^{-1}). So, there was a remarkable chance for further usage of SSBC in subsequent cycles because it still had a lot of free available active sites after the first sorption (cycle 1). It was evident that regeneration of the sorbent from the two oppositely charged dyes had a negligible decline which was confirmed by the high removal % of SSBC sorbent exceeded 87% up to the fourth cycle for both dyes sorption process. So SSBC can be considered as a promising and excellent sorbent for CV and CR dyes removal.

Comparison the sorption of cationic and anionic dyes with different sorbents

Sorption performance of different sorbents depends on many factors such as chemical composition, porosity, surface area and total surface charge. Several sorbents were investigated for dyes removal. A direct comparison of sorption performance is difficult because of different experimental conditions; however, this is a useful criterion for judging the potential of synthesized sorbent to have the priority for using. Tables S4 and S5 (see Supplementary Material) shows a

Table 6 Removal (%) of CV and CR dyes from spiked tap and wastewater samples using SSBC sorbent

Spiked samples		Spiked tap water				Spiked Wastewater			
Dyes concentration (mg L^{-1})		5	10	15	20	5	10	15	20
CV	Removal (%)	90.4	88.8	87.8	86.1	88.2	87.3	86.4	85.2
	Sorption capacity (mmol g^{-1})	0.007	0.014	0.021	0.028	0.007	0.014	0.021	0.027
CR	Removal (%)	93.6	92.5	89.3	87.5	90.4	88.8	87.1	86.6
	Sorption capacity (mmol g^{-1})	0.004	0.008	0.012	0.016	0.004	0.008	0.012	0.016

comparison of maximum sorption capacities values established for CV and CR dyes removal by using SSBC and other sorbents. It is noteworthy that SSBC had superior ability compared with other as it had a very fast sorption rate with high sorption capacities towards both CV and CR dyes. Therefore, the SSBC could be used as a promising sorbent in a practical application for CV and CR dyes removal.

Application of SSBC for cationic and anionic dyes extraction from spiked water samples

Real evaluation for the possible use of SSBC as a color removing material from real wastewater samples was performed to confirm sorbent applicability for industrial application (Fig. 8). Table S6 (see Supplementary Material) shows the chemical analysis for wastewater sample collected from petrochemical plant discharge, Port Said, Egypt. In spite of the high conductivity, TDS and total hardness that characterize of wastewater sample, admirable sorption character of SSBC for both CV and CR was recorded. Its removal % exceeded 85% from eight spiked real water samples (Table 6). Accordingly, SSBC sorbent is considered as an efficient sorbent for removing different organic dyes – laden wastewater.

Conclusion

The overarching target of the present work was the preparation of ecofriendly sorbent based on neglected biowastes. On the perspective, wastes as wealth, SSBC was synthesized based on useless available *Sepia pharaonis* shells. Prepared sorbent was characterized by FT-IR, SEM, EDX, pH_{PZC} and BET surface area analyses. Effect of different parameters such as pH, sorbent dose, initial concentration, temperature, contact time, ionic strength and microwave radiation on sorption process was carried out. The results showed that SSBC had maximum sorption capacities reached to 0.536 mmol g^{-1} (218.67 mg g^{-1}) and 0.359 mmol g^{-1} (250.10 mg g^{-1}) for CV and CR dyes, respectively. The sorption is monolayer, endothermic controlled PSORE. The microwaved enforced sorption increases mass transfer and reduces saturation time to less than 1 min. The recyclability of SSBC was successfully achieved after four repeated cycles. Applicability of SSBC to be used as a sorbent for CV and CR dyes removal from spiked tap water and wastewater samples was successfully achieved with removal % exceeded 85%. Accordingly, the present study provides a model for recycling untapped sepia shells to be exploited as a cleaning tool for amputation of cationic and anionic dyes.

Compliance with ethical standards

Conflict of interest The authors confirm that there are no known conflicts of interest associated with this publication and there has been no significant financial support for this work that could have influenced its outcome.

References

1. Calero M, Rodríguez II, Pérez A, Lara MA, Blázquez G. Neural fuzzy modelization of copper removal from water by biosorption in fixed-bed columns using olive stone and pinion shell. Bioresour Technol. 2018;252:100–9.
2. Li Y, Bai P, Yan Y, Yan W, Shi W, Xu R. Removal of Zn^{2+}, Pb^{2+}, Cd^{2+}, and Cu^{2+} from aqueous solution by synthetic clinoptilolite. Microporous Mesoporous Mater. 2019;273:203–11.
3. Jacob JM, Karthik C, Saratale RG, Kumar SS, Prabakar D, Kadirvelu K, et al. Biological approaches to tackle heavy metal pollution: a survey of literature. J Environ Manag. 2018;217:56–70.
4. Zhang J, Li F, Sun Q. Rapid and selective adsorption of cationic dyes by a unique metal-organic framework with decorated pore surface. Appl Surf Sci. 2018;440:1219–26.
5. Zeng L, Xiao L, Long Y, Shi X. Trichloroacetic acid-modulated synthesis of polyoxometalate@UiO-66 for selective adsorption of cationic dyes. J Colloid Interface Sci. 2018;516:274–83.
6. Narayanan N, Gupta S, Gajbhiye VT, Manjaiah KM. Optimization of isotherm models for pesticide sorption on biopolymer-nanoclay composite by error analysis. Chemosphere. 2017;173:502–11.
7. Alharbi OM. Sorption, kinetic, thermodynamics and artificial neural network modelling of phenol and 3-amino-phenol in water on composite iron nano-adsorbent. J Mol Liq. 2018;260:261–9.
8. De Lima CR, Gomes DN, Filho JR, Pereira MR, Fonseca JL. Anionic and cationic drug sorption on interpolyelectrolyte complexes. Colloids Surf. B. 2018;170:210–8.
9. Raeiszadeh M, Hakimian A, Shojaei A, Molavi H. Nanodiamond-filled chitosan as an efficient adsorbent for anionic dye removal from aqueous solutions. J. Environ. Chem. Eng. 2018;6:3283–94.
10. Aboelfetoh EF, Elhelaly AA, Gemeay AH. Synergistic effect of cu(II) in the one-pot synthesis of reduced graphene oxide (rGO/CuxO) nanohybrids as adsorbents for cationic and anionic dyes. J Environ Chem. 2018;6:623–34.
11. Nishikawa E, Da Silva MG, Vieira MG. Cadmium biosorption by alginate extraction waste and process overview in life cycle assessment context. J Clean Prod. 2018;178:166–75.
12. Novais RM, Ascensão G, Tobaldi DM, Seabra MP, Labrincha JA. Biomass fly ash geopolymer monoliths for effective methylene blue removal from wastewaters. J Clean Prod. 2018;171:783–94.
13. Fontana IB, Peterson M, Cechinel MA. Application of brewing waste as biosorbent for the removal of metallic ions present in groundwater and surface waters from coal regions. J Environ Chem Eng. 2018;6:660–70.
14. Reck IM, Paixao RM, Bergamasco R, Vieira MF, Vieira AMS. Removal of tartrazine from aqueous solutions using adsorbents based on activated carbon and Moringa oleifera seeds. J Clean Prod. 2018;171:85–97.
15. Pellicer JA, López MI, Fortea MI, Hernández JA, Abellán CL, Ros MT, et al. Removing of direct red 83:1 using α- and HP-α-CDs polymerized with epichlorohydrin: kinetic and equilibrium studies. Dyes Pigments. 2018;149:736–46.

16. Dos Santos CC, Mouta R, Junior MC, Santana SA, Silva HA, Bezerra CW. Chitosan-edible oil based materials as upgraded adsorbents for textile dyes. Carbohydr Polym. 2018;180:182–91.
17. Chicinas RP, Bedelean H, Stefan R, Maicaneanu A. Ability of a montmorillonitic clay to interact with cationic and anionic dyes in aqueous solutions. J Mol Struct. 2018;1154:187–95.
18. Kumar PS, Varjani SJ, Suganya S. Treatment of dye wastewater using an ultrasonic aided nanoparticle stacked activated carbon: kinetic and isotherm modeling. Bioresour Technol. 2018;250: 716–22.
19. Bello K, Sarojini BK, Narayana B, Rao A, Byrappa K. A study on adsorption behavior of newly synthesized banana pseudo-stem derived superabsorbent hydrogels for cationic and anionic dye removal from effluents. Carbohydr Polym. 2018;181:605–15.
20. Omer OS, Hussein MA, Hussein BH, Mgaidi A. Adsorption thermodynamics of cationic dyes (methylene blue and crystal violet) to a natural clay mineral from aqueous solution between 293.15 and 323.15 K. Arabian J. Chem. 2018;11:615–23.
21. Fatima M, Farooq R, Lindström RW, Saeed M. A review on biocatalytic decomposition of azo dyes and electrons recovery. J Mol Liq. 2017;246:275–81.
22. Tu NT, Thien TV, Du PD, Chau VT, Mau TX, Khieu DQ. Adsorptive removal of Congo red from aqueous solution using zeolitic imidazolate framework–67. J. Environ. Chem. Eng. 2018;6:2269–80.
23. Aliabadi RS, Mahmoodi NO. Synthesis and characterization of polypyrrole, polyaniline nanoparticles and their nanocomposite for removal of azo dyes; sunset yellow and Congo red. J Clean Prod. 2018;179:235–45.
24. Deng L, Zeng H, Shi Z, Zhang W, Luo J. Sodium dodecyl sulfate intercalated and acrylamide anchored layered double hydroxides: a multifunctional adsorbent for highly efficient removal of Congo red. J Colloid Interface Sci. 2018;521:172–82.
25. Ruan CQ, Strømme M, Lindh J. Preparation of porous 2,3-dialdehyde cellulose beads crosslinked with chitosan and their application in adsorption of Congo red dye. Carbohydr Polym. 2018;181:200–7.
26. Abbasi AR, Karimi M, Daasbjerg K. Efficient removal of crystal violet and methylene blue from wastewater by ultrasound nanoparticles cu-MOF in comparison with mechanosynthesis method. Ultrason Sonochem. 2017;37:182–91.
27. Sarma GK, Gupta SS, Bhattacharyya KG. Adsorption of crystal violet on raw and acid-treated montmorillonite, K10, in aqueous suspension. J Environ Manag. 2016;171:1–10.
28. Mohamed SK, Hegazy SH, Abdelwahab NA, Ramadan AM. Coupled adsorption-photocatalytic degradation of crystal violet under sunlight using chemically synthesized grafted sodium. Int J Biol Macromol. 2018;108:1185–98.
29. Bharagava RN, Mani S, Mulla SI, Saratale GD. Degradation and decolourization potential of an ligninolytic enzyme producing Aeromonas hydrophila for crystal violet dye and its phytotoxicity evaluation. Ecotoxicol Environ Saf. 2018;156:166–75.
30. Sabna V, Thampi SG, Chandrakaran S. Adsorption of crystal violet onto functionalised multi-walled carbon nanotubes: equilibrium and kinetic studies. Ecotoxicol Environ Saf. 2016;134:390–7.
31. Muthukumaran C, Sivakumar VM, Thirumarimurugan M. Adsorption isotherms and kinetic studies of crystal violet dye removal from aqueous solution using surfactant modified magnetic nanoadsorbent. J Taiwan Inst Chem Eng. 2016;63:354–62.
32. Hamoud HI, Finqueneisel G, Azambre B. Removal of binary dyes mixtures with opposite and similar charges by adsorption, coagulation/flocculation and catalytic oxidation in the presence of CeO_2/H_2O_2 Fenton-like system. J Environ Manag. 2017;195: 195–207.
33. Du WN, Chen ST. Photo- and chemocatalytic oxidation of dyes in water. J Environ Manag. 2018;206:507–15.
34. Hosseini SA, Vossoughi M, Mahmoodi NM, Sadrzadeh M. Efficient dye removal from aqueous solution by high-performance electrospun nanofibrous membranes through incorporation of SiO_2 nanoparticles. J Clean Prod. 2018;183:1197–206.
35. Martorell MM, Pajot HF, de Figueroa LI. Biological degradation of reactive black 5 dye by yeast Trichosporon akiyoshidainum. J. Environ. Chem. Eng. 2017;5:5987–93.
36. Ashrafi SD, Rezaei S, Forootanfar H, Mahvi AH, Faramarzi MA. The enzymatic decolorization and detoxification of synthetic dyes by the laccase from a soil-isolated ascomycete. Paraconiothyrium variabile Int Biodeter Biodegr. 2013;85:173–81.
37. Kamani H, Safari GH, Asgari G, Ashrafi SD. Data on modeling of enzymatic elimination of direct red 81 using response surface methodology. Data in Brief. 2018;18:80–6.
38. Mehrabian F, Kamani H, Safari GH, Asgari G, Ashrafi SD. Direct blue 71 removal from aqueous solution by laccase-mediated system; a dataset. Data in Brief. 2018;19:437–43.
39. Ghobashy MM, Elhady MA. pH-sensitive wax emulsion copolymerization with acrylamide hydrogel using gamma irradiation for dye removal. Radiat Phys Chem. 2017;134:47–55.
40. Temesgen F, Gabbiye N, Sahu O. Biosorption of reactive red dye (RRD) on activated surface of banana and orange peels: economical alternative for textile effluent. Surf Interfaces. 2018;12:151–9.
41. Akar ST, Aslan S, Akar T. Conversion of natural mineral to effective geosorbent by coating MnO_2 and its application potential for dye contaminated wastewaters. J Clean Prod. 2018;189:887–97.
42. Di Chen Y, Lin YC, Ho SH, Zhou Y, Ren N. Highly efficient adsorption of dyes by biochar derived from pigments- extracted macroalgae pyrolyzed at different temperature. Bioresour Technol. 2018;259:104–10.
43. Kausar A, Iqbal M, Javed A, Aftab K, Nazli ZI, Bhatti HN, et al. Dyes adsorption using clay and modified clay: a review. J Mol Liq. 2018;256:395–407.
44. León O, Bonilla AM, Soto D, Pérez D, Rangel M, Colina M, et al. Removal of anionic and cationic dyes with bioadsorbent oxidized chitosans. Carbohydr Polym. 2018;194:375–83.
45. Nasiri R, Arsalani N. Synthesis and application of 3D graphene nanocomposite for the removal of cationic dyes from aqueous solutions: response surface methodology design. J Clean Prod. 2018;190:63–71.
46. Toumi KH, Benguerba Y, Erto A, Dotto GL, Khalfaoui M, Tiar C, et al. Molecular modeling of cationic dyes adsorption on agricultural Algerian olive cake waste. J Mol Liq. 2018;264:127–33.
47. Ashrafi SD, Kamani H, Mahvi AH. The optimization study of direct red 81 and methylene blue adsorption on NaOH-modified rice husk. Desalin Water Treat. 2016;57:738–46.
48. Ashrafi SD, Kamani H, Arezomand HS, Yousefi N, Mahvi A.H. Optimization and modeling of process variables for adsorption of basic blue 41 on NaOH-modified rice husk using response surface methodology. Desalin Water Treat 2016; 57: 14051–14059.
49. Rachna K, Agarwal A, Singh NB. Preparation and characterization of zinc ferrite—Polyaniline nanocomposite for removal of rhodamine B dye from aqueous solution. Environ Nanotechnol Monit Manage. 2018;9:154–63.
50. Robles JD, Peresin MS, Tamminen T, Rodríguez A, Larrañeta E, Jääskeläinen AS. Lignin-based hydrogels with "super-swelling" capacities for dye removal. Int J Biol Macromol. 2018;115: 1249–59.
51. Ghaneian MT, Momtaz M, Dehvari M. An investigation of the efficacy of Cuttlefish bone powder in the removal of Reactive Blue 19 dye from aqueous solutions: equilibrium and isotherm studies. J Community Health Res. 2012;1:68–78.
52. Farzana MH, Meenakshi S. Decolorization and detoxification of acid blue 158 dye using cuttlefish bone powder as co-adsorbent via photocatalytic method. J Water Process Eng. 2014;2:22–30.

53. Langmuir I. The adsorption of gases on plane surfaces of glass, mica and platinum. J Am Chem Soc. 1918;40:1361–402.
54. Freundlich HMF. Uber die adsorption in lasungen. Z Phys Chem. 1906;57:385–470.
55. Dubinin MM, Zaverina ED, Radushkevich LV. Sorption and structure of active carbons. I. Adsorption of organic vapors, Zh. Fiz. Khim. 1947;21:1351–62.
56. Temkin MI, Pyzhev V. Kinetics of ammonia synthesis on promoted iron catalysts. Acta physiochim URSS. 1940;12:217–22.
57. Lagergren S. About the theory of so-called adsorption of soluble substances. Kungliga Swenska Vet. 1898;24:1–39.
58. Ho YS, McKay G. Pseudo-second order model for sorption processes. Process Biochem. 1999;34:451–65.
59. Weber WJ, Morris JC. Kinetics of adsorption on carbon from solutions. J Sanit Eng Div ASCE. 1963;89:31–60.
60. Zeldowitsch J. The catalytic oxidation of carbon monoxide on manganese dioxide. Acta Physicochim URSS. 1934;1:364–449.
61. Elgarahy AM, Elwakeel KZ, Elshoubaky GA, Mohammad SH. Untapped Sepia Shell–based composite for the sorption of cationic and anionic dyes. Water Air Soil Pollut. 2019;230:217.
62. AbdEl-Salam AH, Ewais HA, Basaleh AS. Silver nanoparticles 33unctionali on the activated carbon as efficient adsorbent for removal of crystal violet dye from aqueous solutions. A kinetic study. J Mol Liq. 2017;248:833–41.
63. Kumari HJ, Krishnamoorthy P, Arumugam TK, Radhakrishnan S, Vasudevan D. An efficient removal of crystal violet dye from waste water by adsorption onto TLAC/chitosan composite: a novel low cost adsorbent. Int J Biol Macromol. 2017;96:324–33.
64. Ghazali A, Shirani M, Semnani A, Zare-Shahabadi V, Nekoeinia M. Optimization of crystal violet adsorption onto date palm leaves as a potent biosorbent from aqueous solutions using response surface methodology and ant colony. J. Environ. Chem. Eng. 2018;6:3942–50.
65. Bouras HD, Yeddou AR, Bouras N, Hellel D, Holtz MD, Sabaou N, et al. Biosorption of Congo red dye by *Aspergillus carbonarius* M333 and *Penicillium glabrum* Pg1: kinetics, equilibrium and thermodynamic studies. J Taiwan Inst Chem Eng. 2017;80:915–23.
66. Zhang J, Yan Z, Ouyang J, Yang H, Chen D. Highly dispersed sepiolite-based organic modified nanofibers for enhanced adsorption of Congo red. Appl Clay Sci. 2018;157:76–85.
67. Tian C, Feng C, Wei M, Wu Y. Enhanced adsorption of anionic toxic contaminant Congo red by activated carbon with electropositive amine modification. Chemosphere. 2018;208:476–83.
68. Shaban M, Abukhadra MR, Khan AAP, Jibali BM. Removal of Congo red, methylene blue and Cr(VI) ions from water using natural serpentine. J Taiwan Inst Chem Eng. 2018;82:102–16.
69. Albadarin AB, Solomon S, Abou Daher M. Walker G. Efficient removal of anionic and cationic dyes from aqueous systems using spent yerba mate "Ilex paraguariensis". J Taiwan Inst Chem Eng. 2018;82:144–55.
70. Miandad R, Kumar R, Barakat MA, Basheer C, Aburiazaiza AS, Nizami AS, et al. Untapped conversion of plastic waste char into carbon-metal LDOs for the adsorption of Congo red. J Colloid Interface Sci. 2018;511:402–10.
71. Mahmoud ME, Nassar AM, Abou Ali SA, Elweshahy SM. Factors optimization of super fast removal of heavy metals from aqueous solution using microwave-enforced sorption on the surface of a novel nano-composite. Sep Purif Technol. 2017;174:493–501.
72. Oh WC, Ullah K, Zhu L, Da Meng Z, Ye S, Sarkar S. Photocatalytic properties under visible light with graphene based platinium selenide nanocomposites synthesized by microwave assisted method. Mater Sci Semicond Process. 2014;25:34–42.
73. Liu Z, Tian J, Zeng D, Yu C, Zhu L, Huang W, et al. A facile microwave-hydrothermal method to fabricate B doped $ZnWO_4$ nanorods with high crystalline and highly efficient photocatalytic activity. Mater Res Bull. 2017;94:298–306.
74. Lee SH, Kim JH. Kinetic and thermodynamic characteristics of microwave-assisted extraction for the recovery of paclitaxel from Taxus chinensis. Process Biochem. 2019;76:187–93.
75. Razzaghi SE, Arabhosseini A, Turk M, Soubrat T, Cendres A, Kianmehr MH, et al. Operational efficiencies of six microwave based extraction methods for orange peel oil. J Food Eng. 2019;241:26–32.
76. Mahmoud ME, Amira MF, Zaghloul AA, Ibrahim GA. High performance microwave-enforced solid phase extraction of heavy metals from aqueous solutions using magnetic iron oxide nanoparticles- protected-nanosilica. Sep Purif Technol. 2016;163:169–72.
77. Gole VL, Priya A. Microwave-photocatalyzed assisted degradation of brilliant green dye: a batch to continuous approach. J. Water Process Eng. 2017;19:101–5.
78. Mahmoud ME, Abdou AE, Shehata AK, Header HM, Hamed EA. Sustainable super fast adsorptive removal of Congo red dye from water by a novel technique based on microwave-enforced sorption process. J Ind Eng Chem. 2018;57:28–36.
79. Mahmoud ME, Amira MF, Zaghloul AA, Ibrahim GA. Microwave-enforced sorption of heavy metals from aqueous solutions on the surface of magnetic iron oxide-functionalized-3-aminopropyltriethoxysilane. Chem Eng J. 2016;293:200–6.
80. Yap MW, Mubarak NW, Sahu JN, Abdullah EC. Microwave induced synthesis of magnetic biochar from agricultural biomass for removal of lead and cadmium from wastewater. J Ind Eng Chem. 2017;45:287–95.
81. Mahmoud ME, Hassan SS, Kamel AH, Elserw MI. Development of microwave-assisted functionalized nanosilicas for instantaneous removal of heavy metals. Powder Technol. 2018;326:454–66.
82. Salih SS, Ghosh TK. Highly efficient competitive removal of Pb(II) and Ni(II) by chitosan/ diatomaceous earth composite. J. Environ. Chem. Eng. 2018;6:435–43.
83. Deniz F, Kepekci RA. A promising biosorbent for biosorption of a model hetero-bireactive dye from aqueous medium. Fibers Polym. 2017;18:476–82.
84. Maaloul N, Oulego P, Rendueles M, Ghorbal A, Díaz M. Novel biosorbents from almond shells: characterization and adsorption properties modeling for cu(II) ions from aqueous solutions. J. Environ. Chem Eng 2017; 5: 2944–2954.
85. Morosanu I, Teodosiu C, Paduraru C, Ibanescu D, Tofan L. Biosorption of lead ions from aqueous effluents by rapeseed biomass. New Biotechnol. 2017;39:110–24.
86. Álvarez-Torrellas S, Ribeiro RS, Gomes HT, Ovejero G, García J. Removal of antibiotic compounds by adsorption using glycerol-based carbon materials. Chem Eng J. 2016;296:277–88.
87. Elwakeel KZ, Elgarahy AM, Mohammad SH. Use of beach bivalve shells located at Port Said coast (Egypt) as a green approach for methylene blue removal. J. Environ. Chem. Eng. 2017;5:578–87.
88. Zhang Z, Shan Y, Wang J, Ling H, Zang S, Gao W, et al. Investigation on the rapid degradation of Congo red catalyzed by activated carbon powder under microwave irradiation. J Hazard Mater. 2007;147:325–33.
89. Bi X, Wang P, Jiao C, Cao H. Degradation of remazol golden yellow dye wastewater in microwave enhanced ClO_2 catalytic oxidation process. J Hazard Mater. 2009;168:895–900.
90. Priyantha N, Lim LB, Tennakoon DT, Liaw ET, Ing CH, Liyandeniya AB. Biosorption of cationic dyes on breadfruit (Artocarpus altilis) peel and core. Appl Water Sci. 2018;8:37.
91. Gunasundari E, Kumar PS. Adsorption isotherm, kinetics and thermodynamic analysis of cu(II) ions onto the dried algal biomass (*Spirulina platensis*). J Ind Eng Chem. 2017;56:129–44.

92. Guo H, Bi C, Zeng C, Ma W, Yan L, Li K, et al. Camellia oleifera seed shell carbon as an efficient renewable bio-adsorbent for the adsorption removal of hexavalent chromium and methylene blue from aqueous solution. J Mol Liq. 2018;249:629–36.
93. You L, Huang C, Lu F, Wang A, Liu X, Zhang Q. Facile synthesis of high performance porous magnetic chitosan-polyethylenimine polymer composite for Congo red removal. Int J Biol Macromol. 2018;107:1620–8.
94. Mouni L, Belkhiri L, Bollinger JC, Bouzaza A, Assadi A, Tirri A, et al. Removal of methylene blue from aqueous solutions by adsorption on kaolin: kinetic and equilibrium studies. Appl Clay Sci. 2018;153:38–45.
95. Rangabhashiyam S, Lata S, Balasubramanian P. Biosorption characteristics of methylene blue and malachite green from simulated wastewater onto *Carica papaya* wood biosorbent. Surf. Interfaces. 2018;10:197–215.
96. Munagapati VS, Yarramuthi V, Kim Y, Lee KM, Su KD. Removal of anionic dyes (reactive black 5 and Congo red) from aqueous solutions using Banana Peel powder as an adsorbent. Ecotoxicol Environ Safe. 2018;148:601–7.
97. Siddiqui SH. The removal of Cu^{2+}, Ni^{2+} and methylene blue (MB) from aqueous solution using Luffa Actangula carbon: kinetics, thermodynamic and isotherm and response methodology. Groundwater Sustainable Dev. 2018;6:141–9.
98. Foo KY, Hameed BH. Factors affecting the carbon yield and adsorption capability of the mangosteen peel activated carbon prepared by microwave assisted K_2CO_3 activation. Chem Eng J. 2012;180:66–74.
99. Mandal V, Mandal SC. Design and performance evaluation of a microwave based low carbon yielding extraction technique for naturally occurring bioactive triterpenoid: Oleanolic acid. Biochem Eng J. 2010;50:63–70.
100. Chan CH, Yusoff R, Ngoh GC, Kung FW. Microwave-assisted extractions of active ingredients from plants. J Chromatogr A. 2011;1218:6213–25.
101. Mbarki F, Kesraoui A, Seffen M, Ayrault P. Kinetic, thermodynamic, and adsorption behavior of cationic and anionic dyes onto corn stigmata: nonlinear and stochastic analyses. Water Air Soil Pollut. 2018;229:95.
102. Demey H, Vincent T, Guibal E. A novel algal-based sorbent for heavy metal removal. Chem Eng J. 2018;332:582–95.